JACS
JOURNAL OF THE AMERICAN CHEMICAL SOCIETY

COMMUNICATION

pubs.acs.org/JACS

Site-Specific Measurement of Slow Motions in Proteins

Józef R. Lewandowski,[†,∥] Hans Jürgen Sass,[‡] Stephan Grzesiek,[‡] Martin Blackledge,[§] and Lyndon Emsley*[,†]

[†]Université de Lyon, CNRS/ENS-Lyon/UCB-Lyon 1, Centre de RMN à Très Hauts Champs, 69100 Villeurbanne, France

[‡]Biozentrum, University of Basel, 4056 Basel, Switzerland

[§]Protein Dynamics and Flexibility, Institut de Biologie Structurale Jean Pierre Ebel, UMR 5075, CNRS/CEA/UJF, 38027 Grenoble, France

Supporting Information

ABSTRACT: We demonstrate that a quantitative measure of slow molecular motions in solid proteins can be accessed by measuring site-specific ^{15}N rotating-frame relaxation rates at high magic-angle-spinning frequencies.

Protein motions occurring on the nano- to millisecond time scale are often of great functional relevance. However, currently no method can simultaneously measure atom-specific amplitudes and time scales of molecular motions occurring on time scales similar to or longer than the overall rotational diffusion times in solution (the limit for NMR relaxation measurements in solution). The amplitude of motions in the nano- to millisecond range can be obtained quantitatively from residual dipolar coupling-based measurements in anisotropic solutions.[1] However, such methods yield only an upper bound for the time scale of the molecular motions. Site-specific spin−spin T_2 relaxation times obtained in the solid state in combination with spin−lattice T_1 relaxation times[2,3] could in principle yield both amplitudes and time scales of slow molecular motions. Exploiting this unique potential has not been possible to date because of the lack of reliable methods for measuring T_2 relaxation times.

The primary challenge for measuring ^{15}N (or ^{13}C) T_2 as a probe of dynamics in proteins in the solid state is the separation of incoherent (relaxation resulting from stochastic modulations of local fields by molecular motions; for clarity, we reserve the term "relaxation" exclusively for such processes) and coherent (e.g., dipolar dephasing) contributions to the decay rate of transverse magnetization.[4,5] With typical settings in a fully protonated protein, the coherent contribution dominates the coherence lifetimes, usually preventing access to quantitative motional information. It has been shown for perdeuterated proteins with ≤10% of the amide protons back-exchanged, that it is possible, at least in principle, to obtain an estimate of T_2-related parameters through a measurement of ^{15}N dipole chemical shift anisotropy (CSA) cross-correlated relaxation.[6] Since the coherent dipolar dephasing contributes in a similar way to the decay of both components of the J_{NH} multiplet, overestimation of spectral density $J_0(0)$ is minimized because the motional information is encoded in the difference of the two rates rather than their absolute values. Unfortunately, for the cross-correlated relaxation rates to yield a meaningful motional constraint, the measurement has to be very precise because the errors for decay rates for each component cumulate. Furthermore, to date there is no approach that would yield incoherent ^{15}N and ^{13}C T_2 values in fully protonated proteins.

Here we demonstrate that, surprisingly, a reliable measure of the site-specific incoherent T_2 can be obtained even in fully protonated proteins by measuring $T_{1\rho}$ for samples undergoing magic-angle spinning (MAS) at frequencies >45 kHz without additional heteronuclear decoupling. Under these conditions, the coherent residual (the difference between the observed rate constant and the rate constant due to relaxation processes) is reduced to <0.27 Hz. Moreover, we use the site-specific values we measured for the protein GB1 to provide quantitative order parameters and correlation times for the NH vector motion.

First we consider the expected values for the incoherent T_2 and estimate the extent to which coherent dipolar dephasing contributes to the ^{15}N coherence lifetimes in hydrated proteins under a range of typical experimental conditions. For relatively rigid proteins with a compact fold, we can estimate the expected range of values for the incoherent contribution to the transverse magnetization decay time constant by back-calculating T_2 on the basis of molecular motions predicted using other methods. A good crystalline model system is the SH3 domain of chicken α-spectrin. Figure 1 shows the expected bulk T_2 [the blue line is an upper limit based on a fit of only ^{15}N T_1 (the incoherent T_2 should not be longer than this value, as T_1 is rather insensitive to slower motions), and the dashed gray line predicts the bulk T_2 based on data in ref 7; see the Supporting Information (SI) for details] compared with the measured bulk[10] T_2' (where T_2' is the time constant for transverse magnetization decay during a spin echo, which notably refocuses inhomogenous broadening[11]). The figure shows that regardless of the level of dilution of protons and the MAS frequency, the T_2' values measured without decoupling are substantially shorter than predicted for the incoherent T_2 of ∼525 ms (gray line). This means that even in a perdeuterated 10% back-exchanged sample at a MAS frequency of 60 kHz, *the coherent contribution still dominates the ^{15}N coherence lifetimes.* The coherent residual is reduced by applying heteronuclear decoupling, but even with state-of-the-art in instrumentation and methodology, this is still far from sufficient to reach the incoherent/relaxation limit. For example, with the application of heteronuclear decoupling, the bulk ^{15}N T_2' measured in perdeuterated 10% back-exchanged SH3 increases by almost a factor of 2 but is still almost 2 times shorter than the expected lower credible value of incoherent T_2.

Since in the absence of chemical shift exchange, on-resonance $T_{1\rho}$ and T_2 are essentially the same in the limit of weak

Received: July 21, 2011
Published: September 17, 2011

dx.doi.org/10.1021/ja206815h | J. Am. Chem. Soc. 2011, 133, 16762–16765

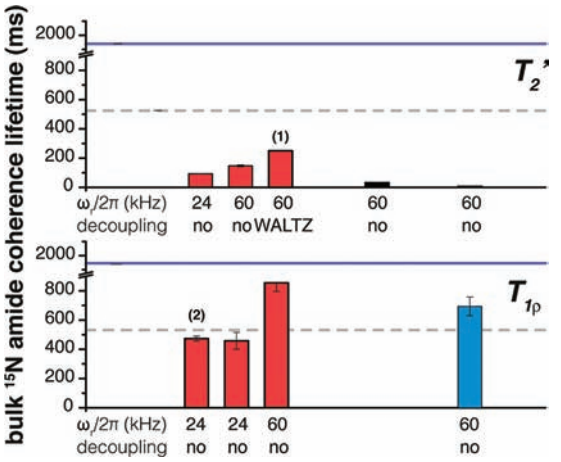

Figure 1. Bulk amide ^{15}N coherence lifetimes for crystalline α-spectrin SH3. Red, black, and blue columns indicate measurements in 10% H_2O/90% D_2O [U-^{2,13}C,^{15}N]SH3, 100% H_2O [U-^{2}H,^{13}C,^{15}N]SH3, and 100% H_2O [U-^{13}C,^{15}N]SH3, respectively, where the percentages refer to the water content in the recrystallization solution. The blue line indicates the predicted upper limit for bulk values of incoherent T_2 based on T_1 measurements and the dashed gray line the predicted bulk T_2 based on all of the data in ref 7 (see the SI for details). All measurements were performed at $\omega_{0H}/2\pi$ = 1 GHz with an effective T_{sample} of 34 °C (as indicated by the bulk H_2O chemical shift[8]), except for (1), where $\omega_{0H}/2\pi$ = 500 MHz and T_{sample} = 23 °C, and (2), where $\omega_{0H}/2\pi$ = 400 MHz and T_{sample} = 27 °C.[9] (2) is a decay constant for an average curve yielded by a sum of individual curves for site-specific on-resonance $T_{1\rho}$ in ref 9. Sample spinning frequencies are indicated below each bar. Further experimental details are outlined in the SI.

radiofrequency (rf) fields, $T_{1\rho}$ is often used in solution-state NMR experiments to obtain an estimate for T_2.[12] Site-specific $T_{1\rho}$ was proposed as a probe of micro- to millisecond motions in the solid state for perdeuterated and 10−20% back-exchanged microcrystalline SH3. As shown in Figure 1, the average $T_{1\rho}$ values reported for 10% H_2O [U-^{13}C,^{15}N,^{2}H]SH3 in ref 9 for sample spinning at $\omega_r/2\pi$ = 24 kHz are similar to our bulk measurements under similar conditions but at 1 GHz. Notably, however, both the average of the reported site-specific measurements and the bulk measurement of 460−470 ms are still slightly less than the prediction of incoherent T_2.

Here we show that, unexpectedly, the situation changes dramatically when we perform the measurement at higher spinning frequencies, where the coherent residual is averaged even further. The same $T_{1\rho}$ measurement on 10% H_2O [U-^{13}C,^{15}N,^{2}H]-SH3 but now using 60 kHz sample spinning yields bulk time constants of 855 ± 60 ms, well above the predicted lower limit for incoherent T_2. It is even more remarkable that the same measurement on fully protonated [U-^{13}C,^{15}N]SH3 gives a bulk $T_{1\rho}$ of 696 ± 64 ms, also well above the predicted value for incoherent T_2 based on T_1, η_{DDxCSA}, and S^2_{NH} data ($T_{1\rho}$ in fully protonated samples is expected to be slightly shorter than in perdeuterated samples because of contributions from protons that are not directly bonded, which increase the overall observed rate by several percent; even if we neglect these protons, the difference yields an average upper bound of 0.27 Hz for the coherent residual). This suggests that combination of fast MAS and relatively weak ^{15}N spin-lock fields is sufficient to render the coherent contribution insignificant in the transverse decay rate of ^{15}N, even in fully protonated proteins.

At first it may not be obvious why the coherent residual should be "decoupled" so much more efficiently in a $T_{1\rho}$ than in a T_2'

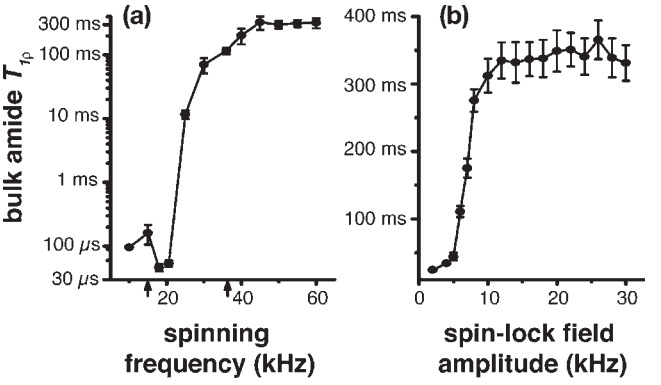

Figure 2. Measured bulk amide ^{15}N $T_{1\rho}$ in [U-^{13}C,^{15}N]GB1 at $\omega_{0H}/2\pi$ = 500 MHz with T_{sample} = 24 °C [based on $\delta(H_2O)$[8]] (a) as a function of spinning frequency with $\omega_{1N}/2\pi$ = 18 kHz and (b) as a function of spin-lock field amplitude at $\omega_r/2\pi$ = 60 kHz. The ^{15}N spin-lock fields were calibrated from rotary resonance conditions and then scaled linearly. No ^{1}H decoupling was used during the ^{15}N spin-lock. Arrows in (a) indicate rotary resonance conditions where there is an additional coherent contribution to the decay due to dipolar/CSA recoupling.

measurement. As shown in Figure S1 in the SI, we find that this is clearly due to spin dynamics induced by ^{1}H−^{1}H dipolar couplings, which do not lead to significant dephasing in a $T_{1\rho}$ measurement but play a critical role in a T_2' echo experiment.

We confirm that the measured values are dominated by the incoherent contribution by making sure they no longer depend on experimental parameters such as the amplitude of the spin-lock field or the sample spinning rate. Figure 2a shows measured bulk amide ^{15}N $T_{1\rho}$ values in fully protonated [U-^{13}C,^{15}N]GB1 as a function of the sample spinning frequency. The bulk $T_{1\rho}$ is ∼96 μs for 10 kHz sample spinning and increases with increasing MAS frequency by more than 3 orders of magnitude, reaching a plateau at ∼320 ms for spinning frequencies above 45 kHz. Figure 2b depicts the evolution of the bulk ^{15}N $T_{1\rho}$ as a function of the spin-lock field amplitude for experiments performed with 60 kHz sample spinning. We observe asymptotic behavior for spin-locking fields above 10 kHz. The asymptotic behavior for $T_{1\rho}$ at spinning frequencies above 45 kHz and spin-lock field amplitudes above 10 kHz is a further indication that the coherent residual is essentially eliminated. Moreover, these results indicate that an appropriate way to obtain accurate measures of incoherent T_2, even in fully protonated proteins, is to measure $T_{1\rho}$ with 60 kHz sample spinning using 15−20 kHz spin-lock field amplitudes. Some spin-lock field amplitudes must be avoided to prevent the reintroduction of coherent residuals, which would compromise the incoherent T_2 measurement. For example, coherent residuals increase drastically for spin-lock fields near rotary resonance conditions[13,14] (when $\omega_1 = \omega_r$ or $2\omega_r$) because of dipolar/CSA recoupling, which manifests itself by a decrease in the time constants. Moreover, a slight decrease in $T_{1\rho}$ is also observed for the HORROR condition[15] (when $\omega_1 = \omega_r/2$; the decrease is much more severe for ^{13}C).

The bulk measurements illustrate that in the relaxation limit for fully protonated crystalline proteins the coherence lifetimes may be extremely long. That these rates are sensitive to dynamics is first visible in that the bulk ^{15}N $T_{1\rho}$ in GB1 is a factor of 2.5 times shorter than the analogous value for SH3, indicating that on average slow motions are much more prominent in the former protein. The information content can be fully appreciated in the case of site-specific measurements, where we measure coherence

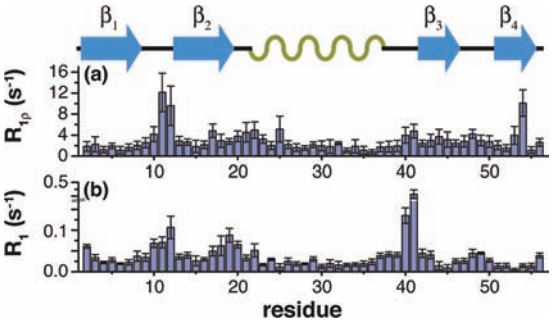

Figure 3. Comparison of amide ^{15}N $R_{1\rho}$ (a) and R_1 (b) measured in [U-^{13}C,^{15}N]GB1 at $\omega_{0H}/2\pi$ = 1 GHz and $\omega_r/2\pi$ = 60 kHz with effective T_{sample} = 25 °C. The ^{15}N $R_{1\rho}$ is an average of measurements performed with spin-lock field amplitudes $\omega_1/2\pi$ = 18 and 23 kHz. No ^{1}H decoupling was used during the spin-lock.

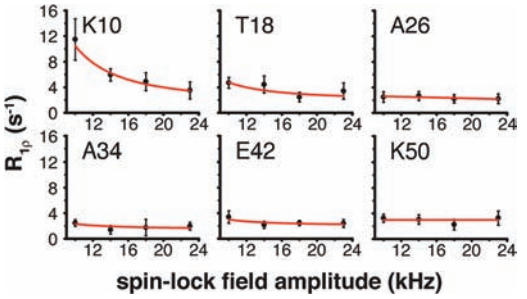

Figure 4. Selected ^{15}N $R_{1\rho}$ dispersion-curve data (every ninth point) measured in [U-^{13}C,^{15}N]GB1. Red curves represent best-fit Lorentzians. Experimental settings are as in Figure 3.

lifetimes of up to 1.2 s. Figure 3a shows site-specific measurements of $R_{1\rho}$ ($R_{1\rho}=1/T_{1\rho}$) in fully protonated [U-^{13}C,^{15}N]-GB1 at 1 GHz ^{1}H Larmor frequency and 60 kHz sample spinning. For comparison we show in Figure 3b the results of ^{15}N R_1 measurements performed under the same experimental conditions. Both $R_{1\rho}$ and R_1 vary significantly between residues, e.g. $R_{1\rho}$ ranges from ~0.82 s^{-1} to ~12 s^{-1} with an average of ~3 s^{-1} (i.e., $T_{1\rho}$ from ~1.2 s to ~82 ms; average ~330 ms). Moreover, as expected, for both measurements the distributions of rates along the protein backbone display similar features, e.g. both rates are elevated in the loop connecting the β_1 and β_2 strands and are relatively low for the C-terminal part of the helix.

The bulk $T_{1\rho}$ dispersion curves in Figure 2b indicate that at 60 kHz sample spinning, $T_{1\rho}$ reaches a plateau above spin-lock field amplitudes of 10 kHz. We measured analogous site-specific $R_{1\rho}$ values ($R_{1\rho} = 1/T_{1\rho}$) as a function of the spin-lock field amplitude over the 10−23 kHz range. Figure 4 shows six examples of the recorded curves (the remaining curves are in Figure S2). In this range, 45 out of 55 backbone amide dispersion curves are flat within experimental error, consistent with the bulk measurement. The fact that the $R_{1\rho}$ values are constant over the explored regime indicates both that decoupling of the coherent residual is adequate and that exchange on time scales between ~40 μs and 0.1 ms is absent for most residues. For the remaining 10 curves, $R_{1\rho}$ decreases monotonically with increasing spin-lock field amplitude, indicating additional <0.1 ms dynamics for those residues. At this stage, it is difficult to determine whether this is an incoherent exchange contribution or a result of interference

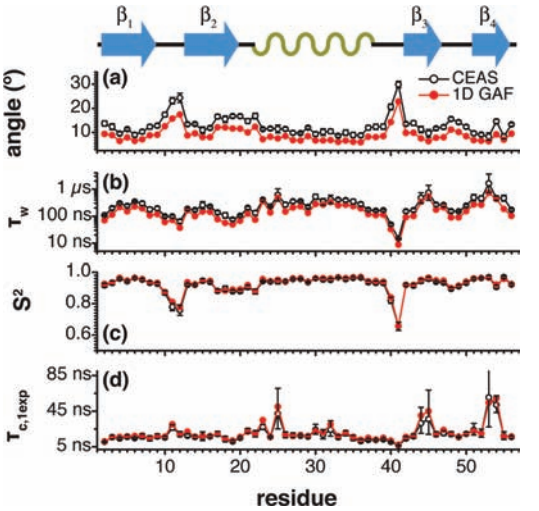

Figure 5. Quantitative analysis of ^{15}N R_1 and $R_{1\rho}$ using CEAS and 1D GAF EAS models: (a) fluctuation angles (θ_0), (b) diffusion times (τ_w), (c) order parameters (S^2), and (d) correlation times ($\tau_{c,1exp}$). For 1D GAF, the NH vector is expressed in the coordinate system defined by the peptide plane (θ = 101.3°,ϕ = 180°, r_{HN} = 1.02 Å)[16] and only fluctuations about the γ axis (defined by the $C_{\alpha,i}-C_{\alpha,i-1}$ vector) are considered. The CSA tensor ($\Delta\sigma$ = −170 ppm, η = 0) is approximated as collinear with dipolar vector. $\tau_{c,1exp}$ in (d) is a single-exponential approximation of the time constant for the correlation functions. Error bars were estimated using Monte Carlo error analysis.

between the dynamics and the averaging of the coherent residual. It is also noteworthy that the ^{15}N spin-lock field plays a critical role in averaging the coherent (heteronuclear) residual. Consequently, $R_{1\rho}$ relaxation dispersion measurements with $\omega_{1N}/2\pi$ < 10 kHz in fully protonated proteins under fast MAS report on a mixture of coherent dephasing and exchange.[24] Moreover, based on the SH3 bulk relaxation measurements, this is true at moderate spinning frequencies even for perdeuterated proteins with only 10% back-exchanged protons. However, in the case of perdeuterated samples, we expect that lower spin-lock fields may be sufficient for quantitative measurements.

We can analyze site-specific measurements of R_1 and $R_{1\rho}$ at a single magnetic field in terms of simple quantitative motional models. Figure 5 shows the results of fitting the experimental data to two motional models combined with the explicit averaged sum approach (EAS): diffusion-in-a-cone (CEAS)[17] and 1D GAF[18] (1D GAF EAS[19]). EAS takes into account the fact that the relaxation rates are orientation-dependent and the relaxation curves multiexponential. Figure 5a,b shows fluctuation angles and diffusion times fitted using both models. To facilitate comparison of the motional amplitudes between the models, Figure 5c indicates the order parameters corresponding to the determined fluctuation angles.[20,21] To allow a more direct comparison of the time scales of the motions, Figure 5d reports single-exponential approximations of the time constants for the CEAS and 1D GAF EAS correlation functions [$\tau_{c,1exp}$, not to be confused with the diffusion times $\tau_w = {}^1/_6D_w$, where D_w is the diffusion constant (see Figure 4b); strictly speaking, the correlation functions are not single-exponential). As Figure 5 shows, the two models yield the same S^2 and $\tau_{c,1exp}$ within experimental error.

Figure 6a shows projection of time scales and amplitudes of backbone motions onto the structure of GB1. The β_1 and β_2 strands on average display faster motions than β_3 and β_4, β_4

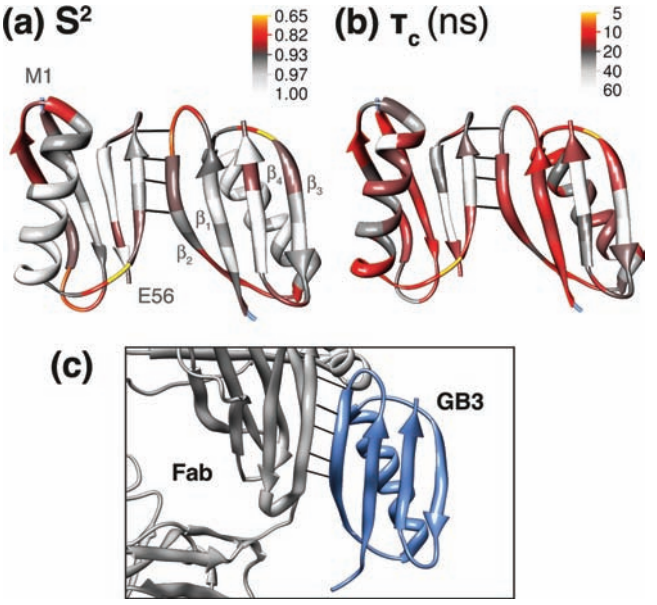

Figure 6. Projection of (a) order parameters (S^2) and (b) correlation times ($\tau_{c,1exp}$) onto a fragment of GB1 crystal. (c) Intermolecular H-bonding mimics the binding interaction in the IgG Fab−GB3 complex.[24]

being the slowest [almost a factor of 2 relative to β_1 and β_2 (Figure 6b)]. The order parameters decrease in all strands from the center to the edges. Intriguingly, the intermolecular H-bonding pattern between β_2 and β_3 closely resembles that in the binding interaction between the β_2 strand of GB3 and the Fab fragment of immunoglobulin G (IgG) in a physiological complex (Figure 6c).[22] In this context, it is interesting that the β_2 strand in the presence of such an interaction is characterized on average by the fastest motion (Figure 6b), with the lowest order parameters (see Figure 6a) compared with other strands. Finally, we note that the S^2_{NH} order parameters obtained using this approach are overall somewhat higher than the S^2_{NH} measured using relaxation times in solution.[23] This may be due to either the higher rigidity of proteins in crystals or as yet unidentified systematic effects that are not included and make the two approaches not directly comparable. Validation of the absolute magnitude of S^2_{NH} is beyond the scope of the present work.

In summary, we have presented an approach for measuring transverse relaxation times even in fully protonated proteins in the solid state. We have shown that at spinning frequencies of >45 kHz, a measurement of $T_{1\rho}$ using moderate rf spin-lock field strengths and without additional heteronuclear decoupling yields coherence lifetimes that are dominated by incoherent relaxation and consistent with the results of other relaxation measurements. This approach allows site-specific time scales and amplitudes of slow motions in biomolecules to be studied quantitatively and should be valuable for refining motional models, including models for anisotropic motions.[19] We have also measured relaxation dispersion curves and found that 45 of 55 residues have no significant motions in the 40 μs to 0.1 ms range. Comparison of T_1 and $T_{1\rho}$ measurements leads to site-specific order parameters and motional correlation times that appear to be relevant to protein−protein interactions. Finally, we note that the drastic difference between T_2' and $T_{1\rho}$ indicates that there is still plenty of room for improvement in current state-of-the-art heteronuclear decoupling sequences, as the available coherence lifetimes are much shorter than the relaxation-limited coherence lifetimes.

■ ASSOCIATED CONTENT

Supporting Information. Experimental details, angles between $B_{1,eff}$ and B_0 in $T_{1\rho}$ measurements on GB1, ^{15}N R_1 and $R_{1\rho}$ (including dispersion) measurements on GB1 at 1 GHz, and spin-evolution simulations. This material is available free of charge via the Internet at http://pubs.acs.org.

■ AUTHOR INFORMATION

Corresponding Author
lyndon.emsley@ens-lyon.fr

Present Addresses
[‖]Department of Chemistry, University of Warwick, Coventry CV4 7AL, U.K.

■ ACKNOWLEDGMENT

We thank Hartmut Oschkinat and Anna Diehl for providing the SH3 samples. We acknowledge support from Agence Nationale de la Recherche (ANR PCV 2007 Protein Motion), the Access to Research Infrastructures Activity in the Seventh Framework Program of the EC (BioNMR 261863), and Swiss National Science Foundation Grant 31-132857. J.R.L. acknowledges support from EU IRG (PIRG03-GA-2008-231026).

■ REFERENCES

(1) Salmon, L.; Bouvignies, G.; Markwick, P.; Lakomek, N.; Showalter, S.; Li, D. W.; Walter, K.; Griesinger, C.; Bruschweiler, R.; Blackledge, M. *Angew. Chem., Int. Ed.* **2009**, *48*, 4154.
(2) Giraud, N.; Bockmann, A.; Lesage, A.; Penin, F.; Blackledge, M.; Emsley, L. *J. Am. Chem. Soc.* **2004**, *126*, 11422.
(3) Lewandowski, J. R.; Sein, J.; Sass, H. J.; Grzesiek, S.; Blackledge, M.; Emsley, L. *J. Am. Chem. Soc.* **2010**, *132*, 8252.
(4) Vanderhart, D. L.; Garroway, A. N. *J. Chem. Phys.* **1979**, *71*, 2773.
(5) Akasaka, K.; Ganapathy, S.; Mcdowell, C. A.; Naito, A. *J. Chem. Phys.* **1983**, *78*, 3567.
(6) Chevelkov, V.; Diehl, A.; Reif, B. *Magn. Reson. Chem.* **2007**, *45*, S156.
(7) Chevelkov, V.; Fink, U.; Reif, B. *J. Biomol. NMR* **2009**, *45*, 197.
(8) Cavanagh, J.; Fairbrother, W. J.; Palmer, A. G., III; Skelton, N. J.; Rance, M. *Protein NMR Spectroscopy: Principles and Practice*, 2nd ed.; Academic Press: San Diego, CA, 2006.
(9) Krushelnitsky, A.; Zinkevich, T.; Reichert, D.; Chevelkov, V.; Reif, B. *J. Am. Chem. Soc.* **2010**, *132*, 11850.
(10) For the bulk measurement, the integral over the backbone amide resonances was monitored as a function of relaxation delay.
(11) Lesage, A.; Bardet, M.; Emsley, L. *J. Am. Chem. Soc.* **1999**, *121*, 10987.
(12) Peng, J. W.; Thanabal, V.; Wagner, G. *J. Magn. Reson.* **1991**, *94*, 82.
(13) Oas, T. G.; Griffin, R. G.; Levitt, M. H. *J. Chem. Phys.* **1988**, *89*, 692.
(14) Levitt, M. H.; Oas, T. G.; Griffin, R. G. *Isr. J. Chem.* **1988**, *28*, 271.
(15) Nielsen, N. C.; Bildsoe, H.; Jakobsen, H. J.; Levitt, M. H. *J. Chem. Phys.* **1994**, *101*, 1805.
(16) Lienin, S. F. Eidgenossische Technische Hochschule, 1998.
(17) Giraud, N.; Blackledge, M.; Goldman, M.; Bockmann, A.; Lesage, A.; Penin, F.; Emsley, L. *J. Am. Chem. Soc.* **2005**, *127*, 18190.
(18) Bruschweiler, R.; Wright, P. E. *J. Am. Chem. Soc.* **1994**, *116*, 8426.
(19) Lewandowski, J. R.; Sein, J.; Blackledge, M.; Emsley, L. *J. Am. Chem. Soc.* **2010**, *132*, 1246.
(20) Lipari, G.; Szabo, A. *J. Am. Chem. Soc.* **1982**, *104*, 4546.
(21) Bremi, T.; Bruschweiler, R. *J. Am. Chem. Soc.* **1997**, *119*, 6672.
(22) Wigley, D. B.; Derrick, J. P.; Shaw, W. V. *FEBS Lett.* **1990**, *277*, 267.
(23) Idiyatullin, D.; Daragan, V. A.; Mayo, K. H. *J. Phys. Chem. B* **2003**, *107*, 2602.
(24) Derrick, J. P.; Wigley, D. B. *J. Mol. Biol.* **1994**, *243*, 906.